NASA TECHNICAL MEMORANDUM

NASA TM X-71792

NASA TM X-71792

INSTALLATION AND AIRSPEED EFFECTS ON JET SHOCK-ASSOCIATED NOISE

by U. von Glahn and J. Goodykoontz
Lewis Research Center
Cleveland, Ohio 44135

TECHNICAL PAPER to be presented at
Ninetieth Meeting of the Acoustical Society of America
San Francisco, California, November 4-7, 1975

INSTALLATION AND AIRSPEED EFFECTS ON JET SHOCK-ASSOCIATED NOISE

by U. von Glahn and J. Goodykoontz
Lewis Research Center

ABSTRACT

Experimental acoustic data are presented to illustrate, at model scale, the effect of varying the nozzle-wing installation on shock-associated noise, statically and with airspeed. The variation in installations included nozzle only, nozzle under-the-wing (with and without flaps deflected), and nozzle over-the-wing (unattached flow). The nozzles used were a conical and a 6-tube mixer nozzle with a cold-flow nozzle pressure ratio of 2.1. A 33-cm diameter free jet was used to simulate airspeed. With the nozzle only, shock wave noise dominated the spectra in the forward quadrant, while jet mixing noise dominated in the rearward quadrant. Similar trends were observed when a wing (flaps retracted) was included. Shock noise was attenuated with an over-the-wing configuration and increased with an under-the-wing configuration (due to reflection from the wing surface). With increasing flap deflection (under-the-wing configuration), the jet-flap interaction noise exceeded the shock noise and became dominant in both quadrants. The free jet results showed that airspeed had no effect on shock noise. The free jet noise data were corrected for convective amplification to approximate flight and comparisons between the various configurations are made.

E-8469

INTRODUCTION

The shock waves in an underexpanded supersonic jet interact with the jet turbulence to cause a noise source in addition to that produced by jet mixing (Refs. 1 and 2). This noise source, ignoring any existence of screech (discrete tones caused by acoustic feedback), is broadband but quite peaked. With cold flow and low supersonic nozzle pressure ratios (PR ~ 2.1), shock noise first becomes evident in the forward quadrant. With increasing pressure ratio, the shock noise becomes less directional and also appears in the rear quadrant. A schematic sketch of this phenomena is shown in Fig. 1. The curves shown represent the velocity dependence of the OASPL of the jet noise at several directivity angles and include the shock associated noise at jet Mach numbers greater than 1.0.

In the present study, conducted at the NASA Lewis Research Center, experimental acoustic data are presented to illustrate, at model scale, the effect of varying the nozzle-wing installation on shock-associated noise, statically and with airspeed. The variation in installations include nozzle only, nozzle under-the-wing (UTW), with and without flaps deflected, and nozzle over-the-wing (OTW) with unattached flow. The wing chord was 33 cm with flaps retracted. The nozzles used were a conical and a 6-tube mixer nozzle operated at a cold-flow nozzle pressure ratio of 2.1. The nominal equivalent diameter of these nozzles was 5.1 and

5.8 cm, respectively. The effect of airspeed on shock noise was obtained using a 33-cm diameter free jet described in Ref. 3 to simulate forward velocity. Acoustic data, spectra and overall sound pressure levels, OASPL, were obtained statically and with a free-jet simulated airspeed of 43 m/sec. The free jet OASPL data were corrected for convective amplification to approximate flight.

APPARATUS

Acoustic Test Stand

Free jet. - An outdoor 33-cm diameter free jet (Fig. 2) was used to simulate forward velocity. For this rig, dry cold air was supplied to a 40.6-cm diameter gate valve from the Center's air supply system by way of a 61-cm diameter underground pipe line. A 25.4-cm diameter butterfly valve was used to control the flow. The nozzle centerline was 3.91 m above the ground.

A muffler system installed in the line downstream of the flow control valve attenuated internal noise caused primarily by the flow control valve. Essentially, the muffler system consisted of perforated plates and dissipative type mufflers. The first perforated plate was located immediately downstream of the flow control valve (40-percent open area plate, 2.54-cm diameter holes). The other perforated plates were located at the entrance and exit of the first dissipative mufflers (20-percent open area plates, 0.318-cm diameter holes). Both dissipative mufflers were sections of pipe that contained splitter plates oriented at right angles to one another so that the flow divided into four channels. The internal surfaces of the muffler pipes and the surfaces of the splitter plates were covered with 2.54-cm thick acoustic absorbent material. The second dissipative muffler was located downstream of the last 45° elbow in the airflow line to take advantage of the reflections caused by turning the flow. In addition the system was wrapped externally with fiber glass and leaded vinyl sheet to impede direct radiation of internal noise through the pipe wall. Two screens (0.795-cm mesh) were placed in the air line downstream of the last muffler to improve the flow distribution to the nozzle. Free-jet velocities from 0 to 43 m/sec were used in the present study.

Nozzle flow system. - The flow system for the test nozzles, proceeding downstream, consisted of a flow control valve, two perforated plates, a four-chamber-baffled muffler, a 10.2-cm inlet pipe and, finally, the nozzle. The muffling system removed sufficient internal noise so that it was not significant in the measured far-field noise levels. Pressurized air was supplied at a nominal temperature of about 288 K. Data were obtained at a nozzle pressure ratio of 2.1 (nominal jet velocity of 337 m/sec). Velocities were determined from measured total pressure and temperature using the isentropic equation.

Models

Wing. - A symmetrical 33-cm chord wooden wing was used for most of the work in the present study (Ref. 4). The wing span was 61 cm. In addition, limited data were obtained with a similar, but cambered, wing with flaps used for the work reported in Refs. 5 and 6.

Nozzles. - The nozzles tested consisted of a conical nozzle and a 6-tube mixer nozzle (Ref. 3) mounted on the centerline of the free jet. The conical nozzle nominal diameter was 5.1 cm. The diameter of each tube of the 6-tube nozzle was 2.36 cm, with a nominal 2.7 cm spacing between adjacent tubes. This nozzle had an equivalent total diameter of 5.8 cm. Pertinent installation dimensions of the nozzles relative to the wing are given in Figs. 3 and 4. Note that the conical nozzle with the cambered airfoil section is inclined 5^{o} toward the airfoil chordline (Fig. 4).

A photograph showing a typical nozzle-wing configuration mounted in the free jet is shown in Fig. 5.

PROCEDURE

Far field noise data were taken in the flyover plane for various test configurations. The test procedure was to obtain steady flow conditions for a given total pressure upstream of each nozzle. Three noise data samples were taken at each microphone location. An atmospheric loss correction was applied to the average of the three samples to give lossless sound pressure level data at 3.05 meters.

The noise from the free jet (large nozzle) contributed substantially to the total noise of the system only in the low frequency region of the spectra (below 400 Hz). Therefore, the effect of the free-stream velocity on the noise from the small nozzle-wing configurations is shown only for those frequencies for which the contribution of the free jet to the total noise level can be considered negligible (generally less than 1 dB).

The noise data were measured by twelve 1.27 cm diameter condenser microphones placed at various intervals on a 3.05 m radius circle around the wing-nozzle setup. With the symmetrical wing, data were taken concurrently for both UTW and OTW configurations as indicated in Fig. 6. The center of the microphone circle was located at the exit of both nozzles. The microphone circle was in a horizontal plane 3.91 m above an asphalt surface and perpendicular to the vertically mounted wing. The plane of the microphone circle passed through the nozzle axes. A standard piston calibrator (124±0.2 dB, 250 Hz tone) was used to calibrate the condenser microphones. Wind screens were placed on all microphones. The noise data were analyzed by a one-third octave band spectrum analyzer. The analyzer determined sound pressure level (SPL) spectra reference to 2×10^{-5} N/m^2. Overall sound pressure levels (OASPL) were computed from

the SPL data. No corrections are made to the acoustic data for ground reflections.

BASELINE NOZZLES

Spectra

Nozzle spectra without airspeed. - Typical spectra in the forward and rearward quadrants for the nozzles are shown in Figs. 7 and 8 for zero airspeed. Also shown by the solid curve are shock-free broadband spectra extrapolated from the subsonic data obtained during the studies reported in Ref. 4. For both conical and six-tube mixer nozzles, shock-associated noise is evident at the higher frequencies in the forward quadrant ($\theta = 60^{o}$) as shown by the cross-hatched regions in Figs. 7 and 8. Because of the smaller tube diameters of the six-tube mixer nozzle compared with the conical nozzle diameter, the shock noise is significant only at 20000 hertz (Fig. 8). With the conical nozzle, shock noise occurs at frequencies greater than 5000 hertz (Fig. 7). The peak SPL increase due to shock noise with the conical nozzle at this directivity angle is 10 dB.

With the conical nozzle, shock noise was completely dominated by jet mixing noise at a directivity angle of 140^{o} as indicated in Fig. 7(b). No shock noise is evident with the six-tube mixer nozzle at a directivity angle of 90^{o} (Fig. 8(b)) or elsewhere in the rearward quadrant.

Shock noise spectra without airspeed. - The static spectra in the frequency region of shock noise at various directivity angles are shown in Fig. 9(a) for the conical nozzle. Also shown for comparison by the solid curves in the figure are the limits of the broadband jet mixing spectra, extrapolated from subsonic data, for the same range of directivity angles. The shock noise decreases in magnitude with increasing directivity angle measured from the inlet. Also, the frequency at which the SPL peaks increases with increasing directivity angle.

Similar results were obtained for the six-tube mixer nozzle (Fig. 9(b)); however, the trends noted for the mixer nozzle were limited to the forward quadrant ($\theta < 90^{o}$). Because the shock noise for the six-tube mixer nozzle was generally limited to one or, at most, two 1/3-octave band at the highest frequencies measured herein, the remaining data presentations will be concerned primarily with the conical nozzle configurations. Data for the six-tube mixer nozzle will be introduced only to illustrate particular points or trends that differ from or amplify those evident in the conical nozzle data.

The frequency at which the peak shock noise occurs for static conditions varies with directivity angle and is directly proportional to the jet velocity and inversely to the shock spacing (Ref. 1). Because the data herein are all at the same pressure ratio (i.e., shock spacing and jet velocity are constant), the shock noise frequency shift with directivity angle simplifies to being directly proportional to the jet ve-

locity. The shock noise frequency shift with directivity angle shown in Fig. 9 can be correlated from Ref. 1 by multiplying the frequency by $(1 + M_c \cos \theta)$ where herein M_c is given by $0.62\ U_j/a_o$.

The reduction in SPL with directivity angle, shown in Fig. 9, can be correlated empirically, for the low nozzle pressure ratio data herein, by

$$\text{SPL} - 20 \log(1 + M_c \cos \theta) \qquad (1)$$

The correlation of shock noise in these terms is shown in Fig. 10. At higher nozzle pressure ratios unpublished NASA data and Ref. 1 show that the directivity pattern for the shock noise becomes more uniform and Eq. (1) is not needed.

Airspeed effects on shock noise. - The effect of airspeed on shock noise spectra, obtained with the free jet, is shown in Fig. 11. Also shown for comparison are the spectra for static conditions and curves for the shock-free broadband mixing noise spectra extrapolated from subsonic data. It is apparent that airspeed does not attenuate shock noise, whereas broadband jet mixing noise is attenuated, although somewhat less than would be predicted from the subsonic tests of Ref. 4. With a directivity angle of 120^o, the high frequency shock noise for static conditions is hardly discernible from that for shock-free jet mixing noise (Fig. 11(b)). However, with airspeed the shock noise, because it is not attenuated by airspeed, becomes clearly evident by surfacing above the SPL values for shock-free jet mixing noise. Results similar to those with the conical nozzle, were obtained with the six-tube mixer nozzle.

Overall Sound Pressure Level

The OASPL for the conical nozzle is shown in Fig. 12, with and without airspeed effects (determined with the free jet), as a function of directivity angle. Also shown for comparison are curves for shock-free OASPL values based on extrapolation from subsonic data (Ref. 4). The data in Fig. 12 show that with shock noise, the OASPL in the forward quadrant is significantly larger than that for the shock-free extrapolation of subsonic OASPL values. Furthermore, the attenuation of OASPL due to airspeed is less in the forward quadrant where shock noise dominates a significant portion of the spectra than in the rearward quadrant where jet mixing noise dominates.

With the six-tube mixer nozzle the OASPL in the forward quadrant was not as greatly affected by shock noise as for the conical nozzle. This is because a much smaller portion of the spectra was affected by shock noise (see Fig. 9). As for the conical nozzle, the shock-free extrapolated data for the six-tube mixer nozzle maximizes in the rearward quadrant.

NOZZLE OVER-THE-WING

Spectra

Static conditions. - Representative spectra for nozzle-over-the-wing (OTW) installations with a conical nozzle are shown in Figs. 13 and 14 for directivity angles of 60° and 120°.

In Fig. 13, the OTW spectra obtained with the conical nozzle located off the wing (nozzle lip 4.45 cm above the wing surface) are shown for directivity angles of 60° and 120°. Also shown for comparison are the nozzle-only curve with shock noise and a shock free OTW curve extrapolated from subsonic data given in Ref. 4. It is apparent that with shock noise, the OTW spectra at high frequencies show little acoustic shielding by the wing. With a shock-free OTW configuration, at $\theta = 60^{\circ}$, the high frequency SPL values are as much as 12 dB lower than those measured with shock noise. Even at $\theta = 120^{\circ}$ the shock noise causes higher SPL values than those obtained with shock-free operation.

In Fig. 14, the OTW spectra with shock noise obtained with the conical nozzle located on and off the wing are compared at directivity angles of 60° and 120°. For the on-the-wing condition, the nozzle lip was located 0.159 cm above the wing surface. Also shown are faired curves of the nozzle-only spectra. In comparison with the nozzle-only data, there is more low frequency noise generated with the nozzle on the surface than that with the nozzle away from the surface. This additional noise is caused by the greater surface scrubbing and trailing edge noise generated when the jet flow is in close proximity to the surface compared with that generated when the jet flow is well off the surface. At the mid-frequencies (5000-8000 Hz) the noise, compared with nozzle-only data, is reduced for both nozzle locations by wing-shielding of the shock noise. In the range of 10000 to 20000 hertz, shielding of the shock noise is not observed when the nozzle is located on the surface (Fig. 14(a)). With the nozzle located off the surface, at these frequencies, some shock noise attenuation due to wing shielding was obtained. The differences in shock noise shielding by the wing are attributed to the shock-cell noise source alteration due to the jet flow interaction with the wing surface.

The differences in nozzle-wing installation for the two cases shown in Fig. 14 are reduced in the rearward quadrant (Fig. 14(b)) where the jet mixing noise begins to dominate shock noise.

In general, the effect of an OTW installation with the six-tube mixer nozzle on the shielding of shock noise was similar to that observed with the conical nozzle mounted off the wing surface. Because of the longer shielding surface relative to the individual tube diameter of the six-tube mixer nozzle compared to the conical nozzle configuration, greater attenuation of shock noise was achieved with the mixer nozzle (7 dB at 20 000 Hz) than with the conical nozzle ($3\frac{1}{2}$ dB at 20000 Hz).

Airspeed effects. - The effect of airspeed on the spectra for OTW

configurations with the conical nozzle is shown in Fig. 15 for a directivity angle of 60° in the forward quadrant. Also shown, for comparison, are the nozzle-only data. In the low frequency range, airspeed attenuates jet mixing noise substantially as reported in Ref. 4. The amount of jet mixing noise attenuation is dependent on the proximity of the nozzle to the wing surface. Somewhat greater amounts of attenuation (up to 3 dB in the midfrequency range) are obtained when the nozzle is located off the wing surface rather than on the surface. With the nozzle off the wing surface, substantially the same jet mixing noise spectra are obtained as that with the nozzle-only (Fig. 15(b)).

In the region of shock noise, some reduction in shock noise is noted at the lower shock noise frequencies (6000 to 8000 Hz); however, no noise reductions due to airspeed are observed at the higher frequencies (>10000 Hz). The shock noise reductions at the lower frequencies are believed due to the source alteration caused by the change of the jet shear layer by the airspeed and the consequent altered interaction with the shock wave.

In the rearward quadrant, where jet mixing noise tended to become dominant at the larger directivity angles (>120°), the effect of airspeed on the OTW spectra was substantially similar to that for subsonic jet velocities reported in Ref. 4.

Similar effects of airspeed on the shock noise were obtained with the six-tube mixer nozzle in the OTW configuration as were obtained with the conical nozzle OTW configuration.

Overall Sound Pressure Level

Nozzle-off-wing. - The OASPL directivity pattern is shown in Fig. 16 with the conical nozzle located off the wing surface, with and without airspeed. The measured OTW OASPL data are compared with that for the nozzle-only in Fig. 16(a). For static conditions, the measured OASPL values for the OTW configuration are attenuated in the forward quadrant by up to 3 dB ($\theta = 40°$) from those for the nozzle only due to the acoustic shielding provided by the wing. With increasing directivity angle, the OASPL values for the nozzle only and OTW configuration approached each other until at angles near 120° and greater, coincidence occurred. At these large directivity angles the additional low frequency noise inherent to this OTW configuration at model scale, offset the high frequency shielding benefits, resulting in the same OASPL values for the nozzle only and the OTW configuration. With airspeed, substantially no attenuation occurred with the OTW configuration at directivity angles of 40° and 60°. For the nozzle-only case, some noise reduction (2 dB) with airspeed did occur at these angles. Thus, in the shock noise dominated forward quadrant, the OASPL for the OTW configuration was generally independent of airspeed. In the rearward quadrant, where the shock noise was no longer as dominant as in the forward quadrant, airspeed attenuated the OASPL increasingly more with increasing directivity angles until the

nozzle-only values were reached at angles of 120° and 140°.

The measured OASPL data for the OTW configuration with shock noise are compared with that for shock free jet mixing OTW noise levels, extrapolated from the subsonic data of Ref. 4, in Fig. 16(b). It is apparent that with shock noise, the measured OASPL data are higher in the forward quadrant than that projected from shockless jet mixing noise by up to 5 dB statically and 9 dB with airspeed at a directivity angle of 40°. With increasing directivity angle, the OASPL values with shock noise approach those for shock free conditions. At directivity angles of 120°, coincidence occurs because, for the present model scale and nozzle pressure ratio, shock noise no longer dominates the spectra.

The OASPL variation with directivity angle for the six-tube mixer nozzle in the OTW configuration was not significantly affected by shock noise and is therefore not included herein.

Nozzle-on-wing. - The OASPL data with shock noise for the OTW configuration using the conical nozzle located on the wing surface and the nozzle only as a function of directivity angle are shown in Fig. 17, with and without airspeed. Also shown for comparison, are curves for jet mixing noise only. Although the spectra showed shielding of the jet mixing noise at high frequencies, the additional interaction noise at low frequencies tended to offset these shielding benefits. Consequently, the OASPL for the OTW configuration and nozzle only were substantially the same. Because of the greater jet-surface interaction noise at low frequencies for this configuration compared with the previous OTW configuration, the OASPL noise levels in the forward quadrant are higher, by as much as 2 dB, compared with those shown in Fig. 16(a).

The OASPL for the OTW configuration with shock noise is compared to that without shock noise in Fig. 17(b). It is apparent that with shock noise the OASPL in the forward quadrant is higher, by as much as 6 dB at directivity angles of 40° and 60° than that without shocks. At directivity angles greater than about 90°, the difference in OASPL with and without shock noise vanishes.

NOZZLE UNDER-THE-WING

Spectra

Static conditions. - Representative static spectra for the conical nozzle installed in nozzle under-the-wing (UTW) configurations with flaps retracted (Fig. 3(a)) are shown in Fig. 18 for a directivity angle of 60°. The effect of the proximity of the wing on the spectra in the jet mixing noise region (frequencies below 4000 Hz) is clearly evident by the comparison of data taken with the nozzle close to the wing with that taken with the nozzle away from the wing. The increased levels in the low frequency range of the spectra are related to the source alteration of the jet flow by the wing surface and trailing edge noise. Comparison between OTW and

UTW noise at frequencies below 4000 hertz indicates similar levels. In the shock noise region (frequencies >4000 Hz), however, some increase in noise due to reflection from the wing (1 to 2 dB) is observed. The preceding trends were noted at all directivity angles.

With the six-tube mixer nozzle results similar to those with the conical nozzle were obtained.

Data obtained with flaps deflected for the UTW configuration are shown in Fig. 19. In Fig. 19(a), the spectra are shown for a 20° flap deflection angle at a directivity angle of 60°. Also shown in the figure are curves representing the spectra for the nozzle only. It is apparent that the jet-flap interaction noise, peaking at about 2200 hertz, is at the same level as the shock noise which peaks at about 8000 hertz. The shock noise level with the flaps deflected is about 2 dB higher than the nozzle-only data due to reflections from the wing and flap surfaces. With a flap deflection of 60°, the jet-flap interaction noise level is so high, due to the greater immersion of the flap in the jet flow at this angle than that at 20° (see Figs. 4(b) and (c)), that it obscures any evidence of the shock noise in the spectra. A representative spectrum at a directivity angle of 60° is shown in Fig. 19(b), together with a curve showing the nozzle-only data. It is apparent that the jet-flap interaction noise is at least 5 dB higher than the shock noise.

Airspeed effects. - With an UTW configuration and flaps retracted (Fig. 3(a)), the jet-wing interaction dominated noise at the low and mid frequencies is attenuated by airspeed as shown in Fig. 20. In this figure the spectra of the UTW configurations with a conical nozzle are shown, together with the nozzle-only data, for a directivity angle of 60°. Shock noise, however, as was the case for the OTW configurations, is not attenuated by airspeed. In the rearward quadrant, at directivity angles where jet mixing noise is the dominant noise source, the sound pressure level for these UTW configurations are attenuated by airspeed across the entire frequency range.

Similar results were obtained with the six-tube mixer nozzle in an UTW configuration and flaps retracted (Fig. 3(b)).

The effect of airspeed on the spectra for the UTW configuration with a conical nozzle and flaps deflected 20° (Fig. 4(b)) is shown in Fig. 21. In the region of jet-flap interaction noise (frequencies less than 4000 Hz), the jet-mixing noise level is reduced by up to 6 dB by airspeed; however, as in the case with the flaps retracted, the shock noise is not significantly affected (less than $1\frac{1}{2}$ dB) by airspeed. The apparent small change in the shock noise level with airspeed could be due to a redirection caused by the airflow over the flap surfaces.

With a flap angle of 60°, it was stated in Ref. 6 that forward velocity had little effect on attenuating the subsonic jet-flap interaction noise (<2 dB). Similar results were obtained with the slightly supersonic jet used in the present study. Consequently, the jet-flap interaction

noise obtained for the static case (Fig. 19(b)) was not attenuated sufficiently by airspeed to uncover the shock noise.

Overall Sound Pressure Level

The presence of a wing with flaps retracted caused the static OASPL to be somewhat higher for the two UTW configurations than that for the nozzle-only over the entire range of directivity angles tested as shown in Fig. 22. This increase is primarily due to acoustic reflection from the wing surface. Except at a 30° directivity angle, substantially the same change in OASPL with airspeed was obtained for the nozzle-only and the UTW configurations at any given directivity angle. The change in OASPL with airspeed was least in the forward quadrant where shock noise was largely dominant and greatest in the rearward quadrant where jet mixing noise dominated. The reductions in OASPL that were achieved in the forward quadrant are attributed to attenuation by airspeed of the jet mixing noise portion of the spectra since the shock noise was not attenuated by airspeed. As shown in Fig. 22, for both UTW configurations, the measured OASPL in the forward quadrant was higher than that projected from shock-free subsonic data.

With the six-tube mixer nozzle, the effect of shock noise on OASPL was insufficient to warrant inclusion of data plots; however, the general trends noted for the UTW configuration with the conical nozzle should also apply to the mixer nozzle.

Because the jet-flap interaction noise was the dominant noise source with the flaps deflected for UTW configurations, the OASPL variation with directivity angle showed little shock noise effect. The variation was essentially that determined for subsonic jet velocities given in Ref. 6. In the forward quadrant, the maximum effect of shock noise was less than 1 dB on the OASPL compared with extrapolated shock-free values from subsonic data.

COMPARISONS OF INSTALLATION EFFECTS ON ACOUSTIC CHARACTERISTICS

Static Conditions

A comparison of the acoustic characteristics, in terms of OASPL as a function of directivity angle, for the various conical nozzle configurations without airspeed and flaps retracted are shown in Fig. 23. The UTW configurations, as expected, show the largest OASPL values at all directivity angles. The OTW configuration with the nozzle located off the wing had the lowest OASPL values of the configurations tested. At a 60° directivity angle the UTW configurations were 3½ dB louder than the quietest OTW configuration. The nozzle-only OASPL values generally were at an OASPL level halfway between the UTW and OTW configurations in the forward quadrant. In the rearward quadrant, where jet mixing noise dominated, the OASPL values for all configurations were within 1 to 2 dB; with the UTW configurations being the noisiest due to acoustic reflection

of the jet mixing noise by the wing surface.

Effect of Airspeed

In order to project the airspeed effects on shock-associated noise obtained in the free jet to flight the effect of relative motion of the noise source with respect to the observer must be added to the jet relative velocity effects measured in a free jet. The dynamic effects or convective amplifications applicable to the present work are taken from Ref. 6 and are given by:

$$\Delta OASPL = -40 \log[1 - (U_o/a_o)\cos\theta] \tag{2}$$

for directivity angles at which shock noise dominated (generally forward quadrant) and

$$\Delta OASPL = -60 \log[1 - (U_o/a_o)\cos\theta] \tag{3}$$

for directivity angles at which jet mixing noise dominated (rearward quadrant). It should be emphasized that the preceding adjustment to the data is intended to indicate only a trend attributable to the convective amplification of the OASPL rather than an exact correction. The Doppler effect on frequency is given by

$$f_D = \frac{f}{1 - \left(\frac{U_o}{a_o}\right)\cos\theta} \tag{4}$$

The result of applying the convective amplification corrections to the OASPL values obtained with the free jet is shown in Fig. 24. The effect of these corrections (Eq. (2) and (3)) to the measured OASPL data tend to increase these values in the forward quadrant and attenuate these values in the rearward quadrant.

Finally, a comparison of the static OASPL values with those projected for flight is shown in Fig. 25. In much of the forward quadrant, due to the dominant shock noise that is not attenuated by airspeed, the flight OASPL values are equal to or exceed those measured statically. In the rearward quadrant where jet mixing noise is dominant, significant reductions (up to 7 dB) are achieved for the flight condition. For all configurations the crossover point between the static and flight OASPL curves is in the forward quadrant; i.e., forward of a 90° directivity angle.

Similar trends to those shown in Fig. 25 would be obtained for the UTW configurations with flaps deflected by applying the convective amplification correction to the measured data obtained with airspeed. Because of the dominance of the jet-flap interaction noise, Eq. (2) generally would apply at all directivity angles. The corrected OASPL with flaps

deflected shows little overall effect of shock noise and the OASPL trends with airspeed are similar to those shown in Ref. 6 for subsonic jet velocities.

CONCLUDING REMARKS

This limited study has demonstrated that statically an OTW configuration can shield shock noise. However, the amount of shielding with shock noise appears to be less at a given frequency than that associated with the shielding of jet mixing noise at the same frequency. Furthermore, the shielding of shock noise is a function of nozzle height above the shielding surface or wing. With a conical nozzle effectively on the wing surface no shock noise attenuation due to shielding was obtained with the OTW configuration tested. With an UTW configuration, shock noise was acoustically amplified by the wing in the same manner as jet mixing noise.

The fact that forward velocity does not attenuate shock noise can cause the OASPL in the forward quadrant to be considerably higher than would be predicted from shock-free subsonic data. Thus the level of shock noise relative to jet mixing noise at a given directivity angle is important to an evaluation of flight effects from static data. At higher pressure ratios than used herein, shock noise can also become dominant in portions of the rearward quadrant, further adding to the problems of predicting noise attenuation for flight.

The limited data presented indicate that frequency-wise, shock noise scales with nozzle size in a Strouhal manner. Consequently, shock noise appears at much lower frequencies with increasing nozzle size than the model scale data shown herein. Also the shock noise level increases directly with nozzle size (diameter squared). Thus, for a full-sized engine nozzle, shock noise becomes an important consideration in the calculations of inflight perceived noise levels, particularly since airspeed does not attenuate shock noise.

The beneficial effects of using a mixer nozzle when shock noise is present lies mainly in moving the shock noise spectra (due to the smaller sized tubes or elements in a mixer nozzle) to higher frequencies which hopefully will have less effect on the OASPL particularly for a full-sized nozzle installation. When the shock noise is restricted to very high frequencies relative to the jet mixing noise peak frequency, the OASPL in the forward quadrant will be more responsive to attenuation by forward velocity since these characteristics will be determined more by jet mixing noise than shock noise.

NOMENCLATURE

a_o ambient speed of sound

f 1/3 octave band center frequency

M_c convective Mach number, $0.62\ U_j/a_o$

OASPL overall sound pressure level, dB, re 2×10^{-5} N/m^2

PR nozzle pressure ratio

SPL 1/3 octave band sound pressure level, dB, re 2×10^{-5} N/m^2

U_j jet velocity at nozzle exhaust plane

U_o airspeed

θ directivity angle measured from inlet

Subscript:

D Doppler

REFERENCES

1. Harper-Bourne, M., and Fisher, M. J., "The Noise from Shock Waves in Supersonic Jets." Proc. AGARD Conf. on Noise Mechanisms, AGARD-CP-131, North Atlantic Treaty Org., 1973, pp. 11-1 to 11-13.

2. von Glahn, U., "Correlation of Total Sound Power and Peak Sideline OASPL from Jet Exhausts," AIAA Paper No. 72-643 (June 1972).

3. von Glahn, U., Groesbeck, D., and Goodykoontz, J., "Velocity Decay and Acoustic Characteristics of Various Nozzle Geometries with Forward Velocity," AIAA Paper No. 73-629 (July 1973).

4. von Glahn, U., Goodykoontz, J., and Wagner, J., "Nozzle Geometry and Forward Velocity Effects on Noise for CTOL Engine-Over-the-Wing Concept," presented at the 86th Meeting of the Acoust. Soc. of Am., Los Angeles, Calif., Oct. 30-Nov. 2, 1973.

5. Olsen, W., Dorsch, R., and Miles, J., "Noise Produced by a Small-Scale, Externally Blown Flap," NASA Technical Note TN D-6636 (Mar. 1972).

6. Goodykoontz, J., Dorsch, R., and von Glahn, U., "Forward Velocity Effects on Under-the-Wing Externally Blown Flap Noise," AIAA Paper No. 75-476 (Mar. 1975).

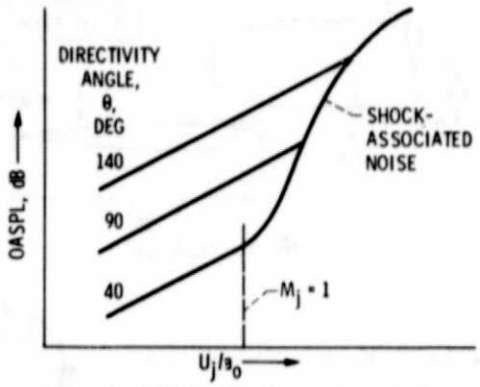

Figure 1. - Velocity dependence of jet noise at several directivity angles showing shock-associated noise (according to reference 1).

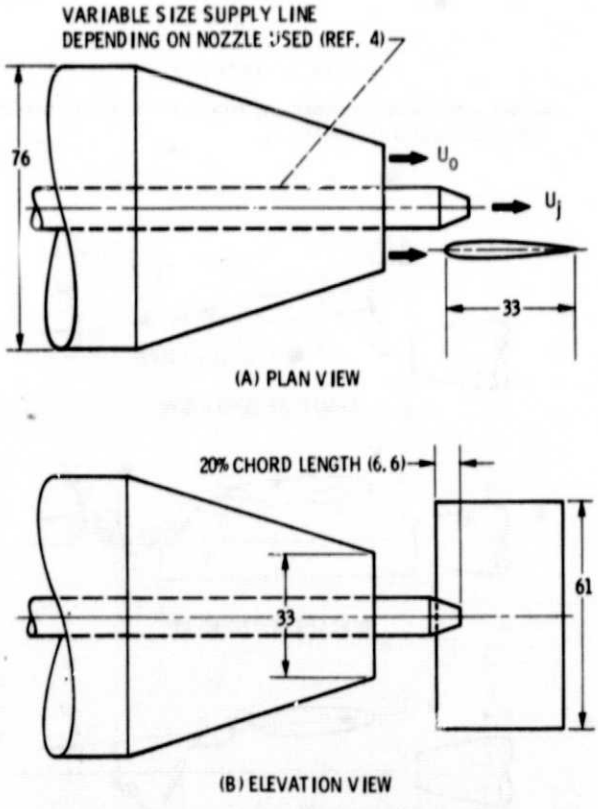

Figure 2. - Schematic of typical nozzle-wing configuration in free jet for acoustic measurements. All dimensions in centimeters.

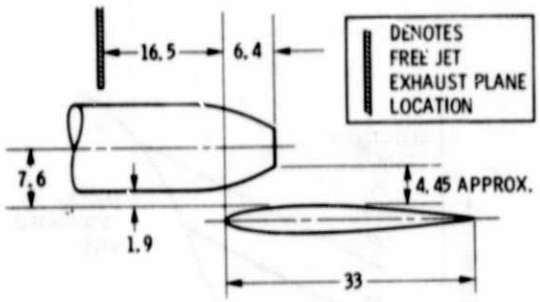

(a) CONICAL NOZZLE.

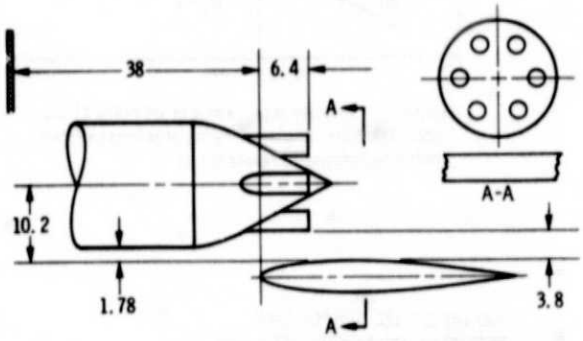

(b) 6-TUBE MIXER NOZZLE.

Figure 3. - Nozzle-wing orientations with symmetrical wing used for both OTW and UTW configurations.

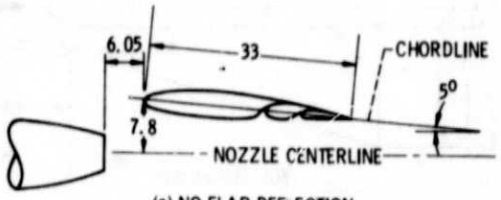

(a) NO FLAP DEFLECTION.

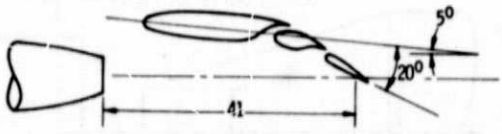

(b) FLAPS DEFLECTED 20°.

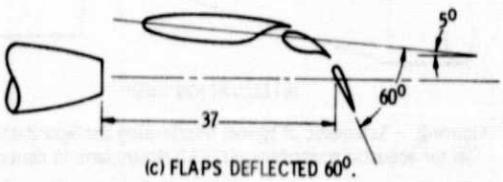

(c) FLAPS DEFLECTED 60°.

Figure 4. - Conical nozzle with wing having flaps (ref. 5).

E-8469

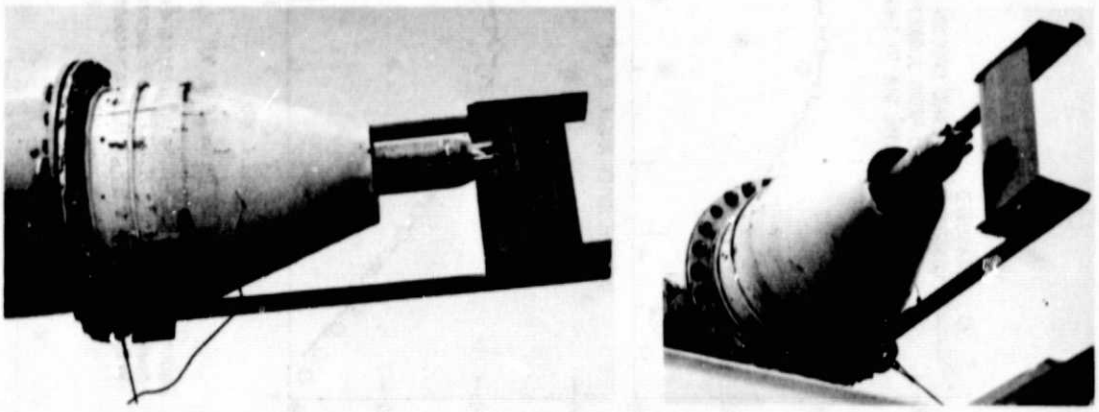

Figure 5. - 6-Tube mixer nozzle with wing installed in free jet.

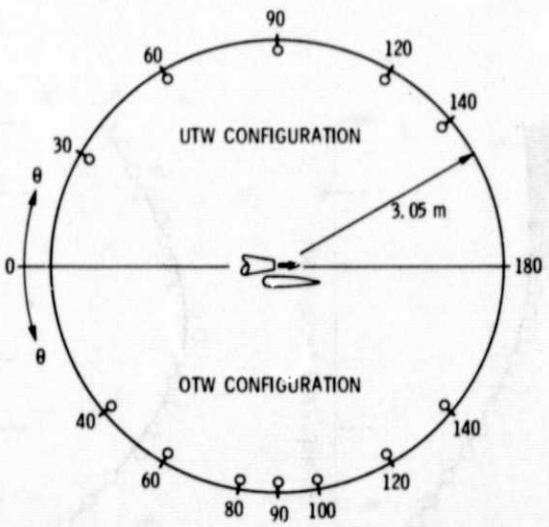

Figure 6. - Microphone layout for UTW and OTW configurations with symmetrical wing. (Simultaneous noise measurements).

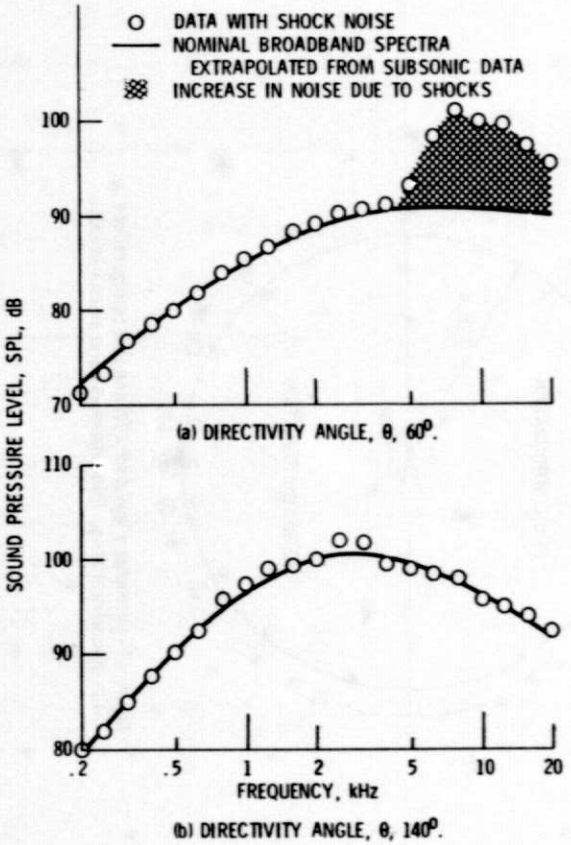

Figure 7. - Sample SPL spectra in forward and rear quadrants for conical nozzle with supersonic jet velocity. U_j, 337 m/sec (PR, 2.1); zero airspeed.

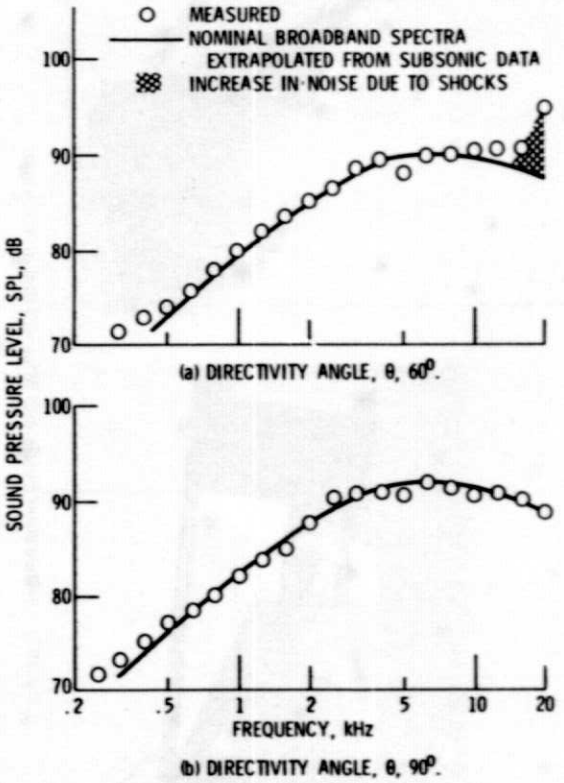

Figure 8. - Sample SPL spectra in forward and rearward quadrants for 6-tube mixer nozzle with supersonic velocity. U_j, 337 m/sec (PR, 2.1); zero airspeed

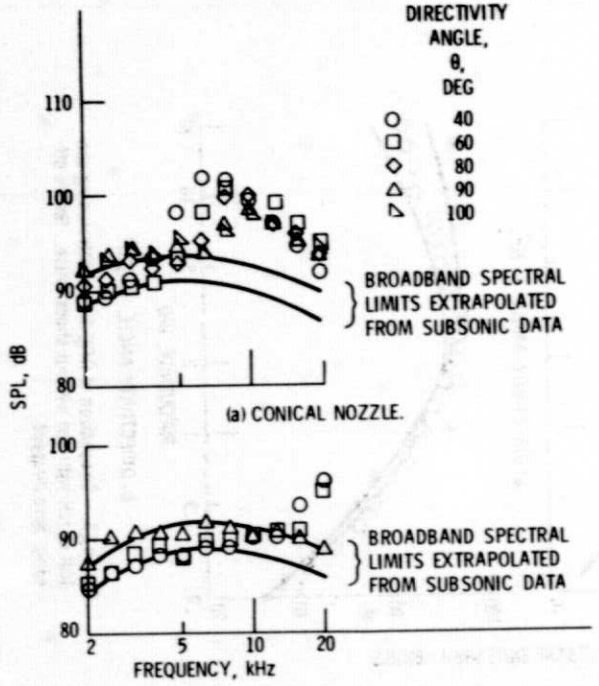

Figure 9. - Shock noise spectra for various nozzles without airspeed for various directivity angles. Nozzle pressure ratio, 2.1.

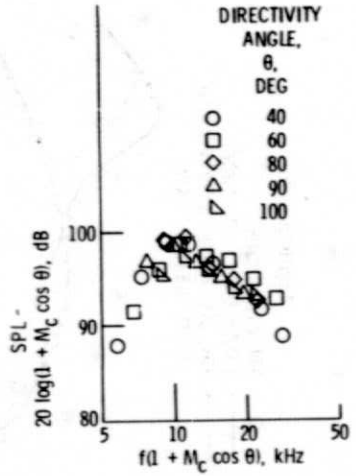

Figure 10. - Conical nozzle shock noise correlation for variations with directivity angle. Nozzle pressure ratio, 2.1; zero airspeed.

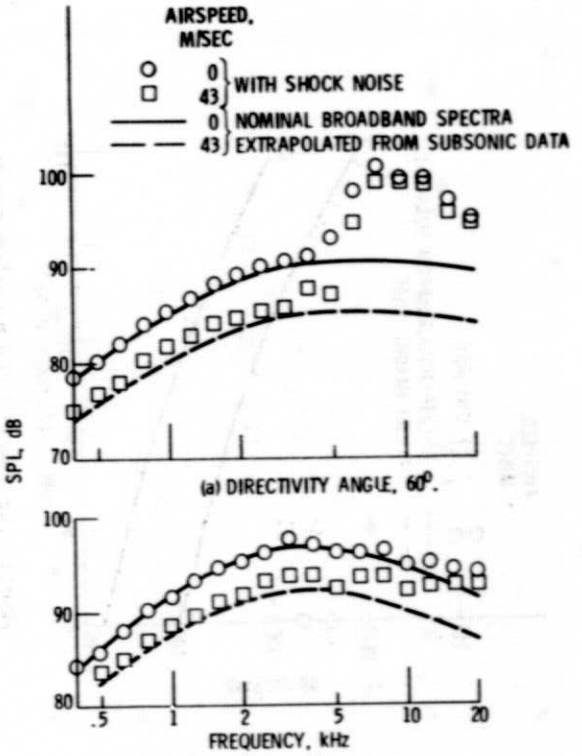

Figure 11. - Comparison of conical nozzle SPL spectra with and without airspeed.

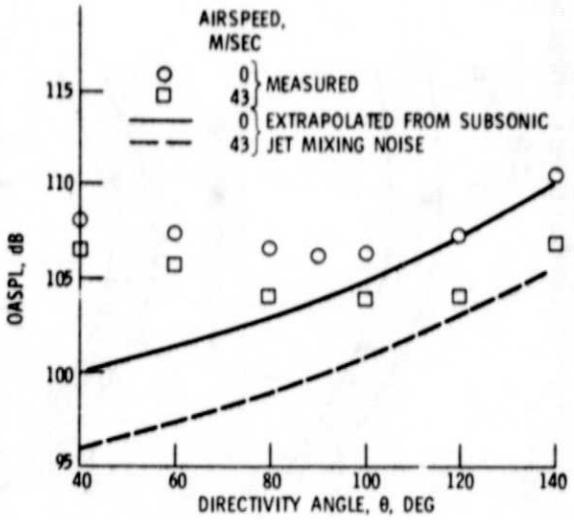

Figure 12. - Variation of OASPL with directivity angle for conical nozzle.

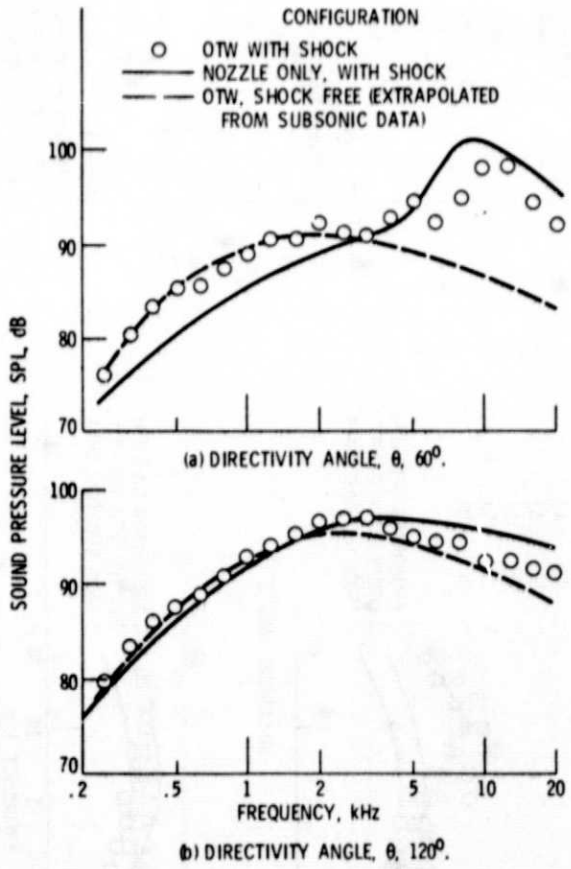

Figure 13. - Comparison of OTW SPL spectra using conical nozzle with and without shock noise. Nozzle off-wing; zero airspeed.

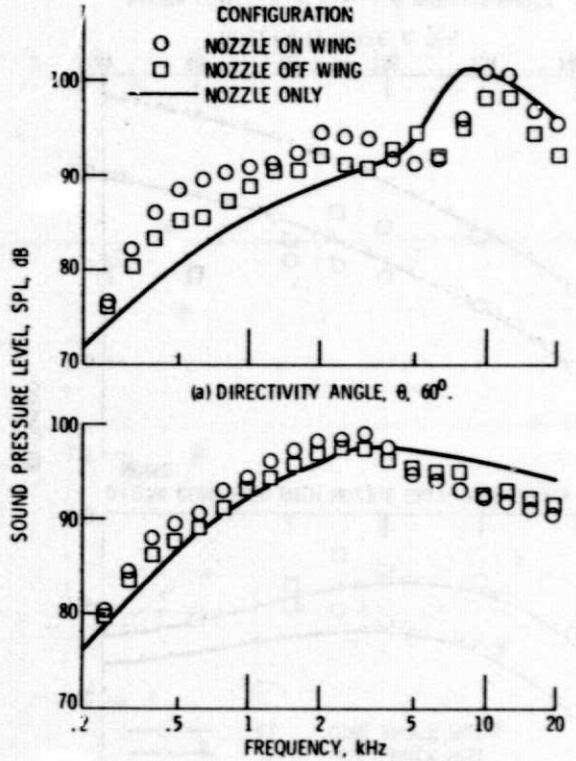

Figure 14. - Comparison of OTW spectra with conical nozzle located on and off the wing. Zero airspeed.

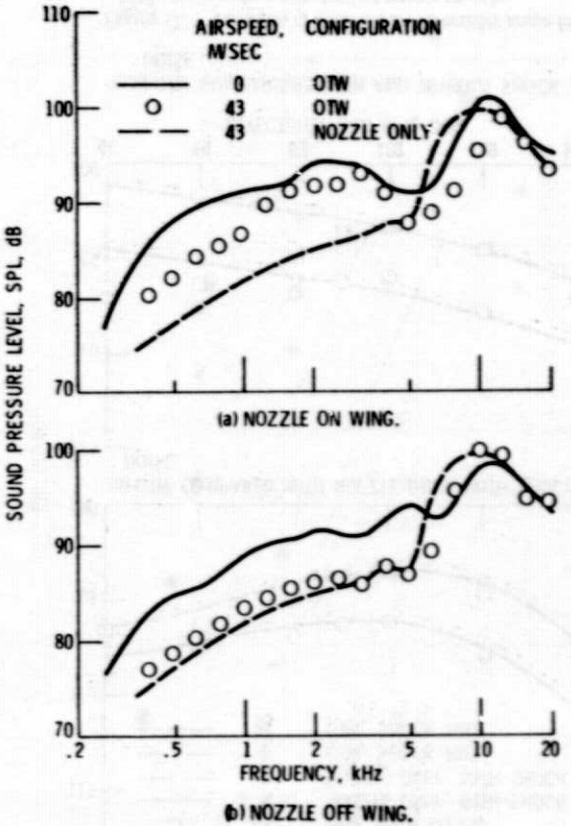

Figure 15. - Comparison of SPL spectra for OTW configuration with and without airspeed. Conical nozzle; directivity angle, 60°.

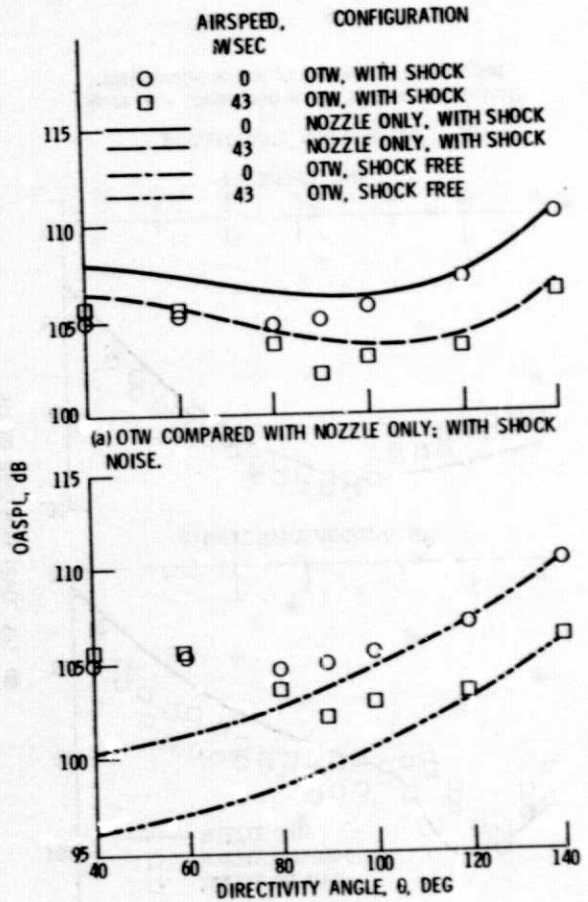

Figure 16. - Variation of OASPL with directivity angle for OTW configuration with conical nozzle off wing.

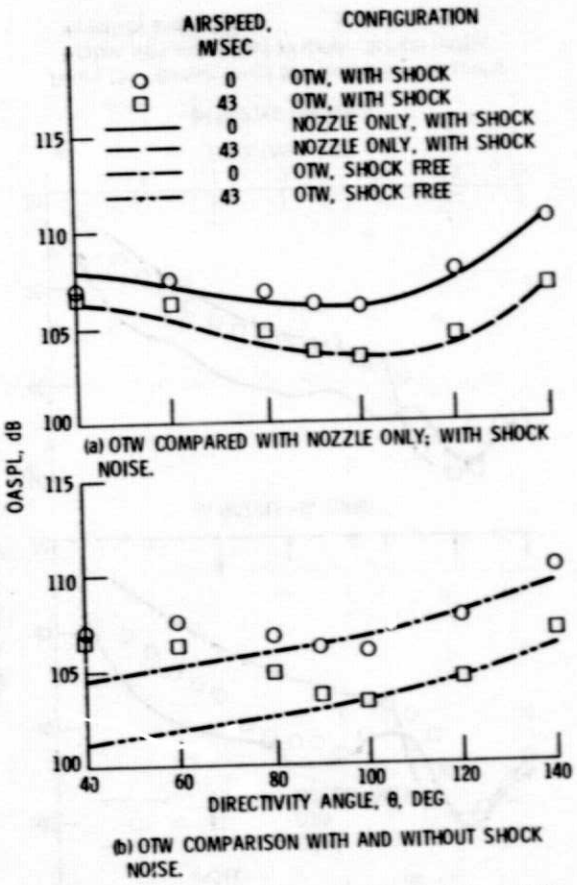

Figure 17. - Variation of OASPL with directivity angle for OTW configuration with conical nozzle on wing.

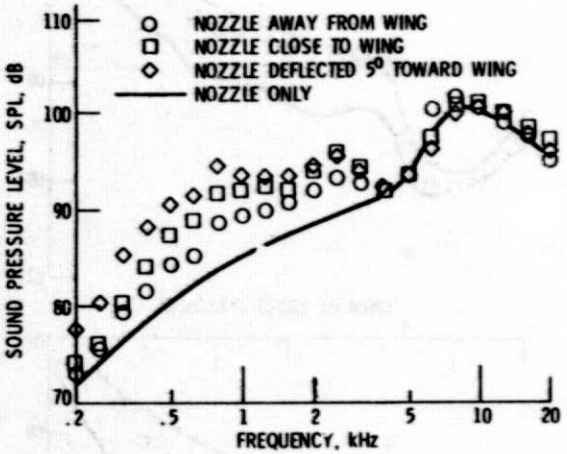

Figure 18. - Typical spectra obtained with conical nozzle in UTW configuration without airspeed. Directivity angle, 60°; flaps retracted.

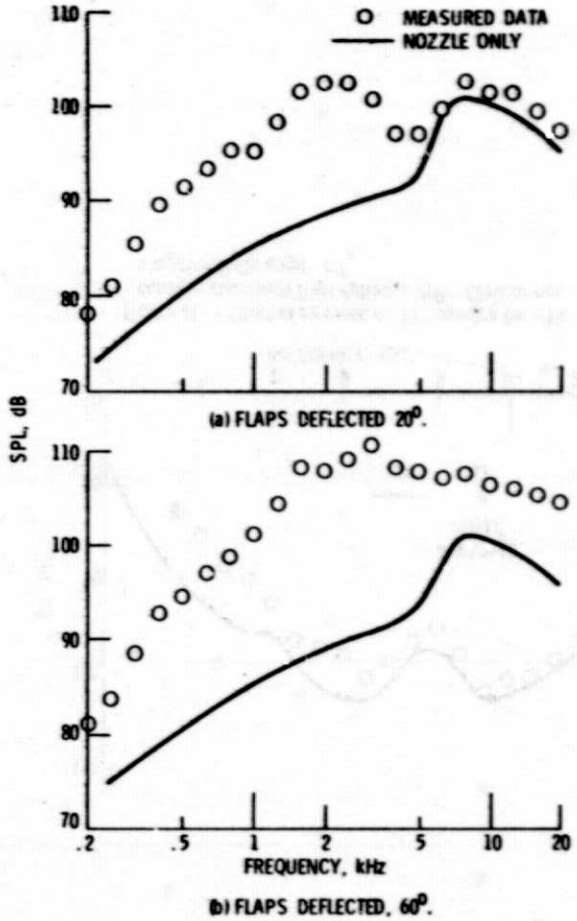

Figure 19. - Typical spectra obtained with conical nozzle and flaps deflected in UTW configuration. Directivity angle, 60°; zero airspeed.

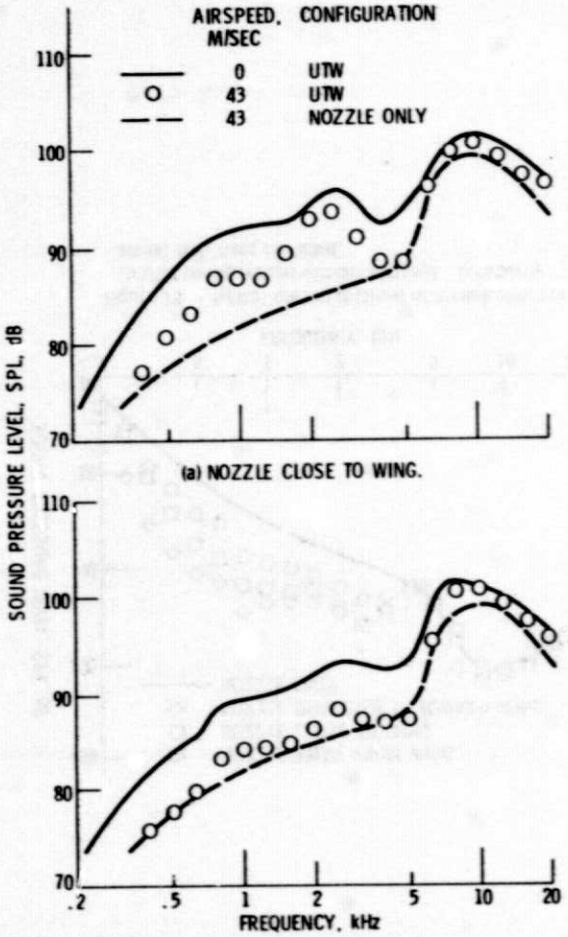

(a) NOZZLE CLOSE TO WING.

(b) NOZZLE AWAY FROM WING.

Figure 20. - Comparison of SPL spectra with and without airspeed for UTW configurations. Conical nozzle and flaps retracted; directivity angle, 60°.

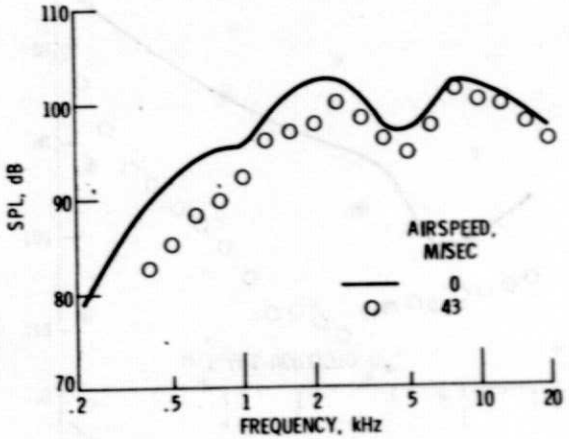

Figure 21. - Effect of airspeed on SPL spectra for UTW configuration with flaps deflected 20°. Conical nozzle; directivity angle, 60°.

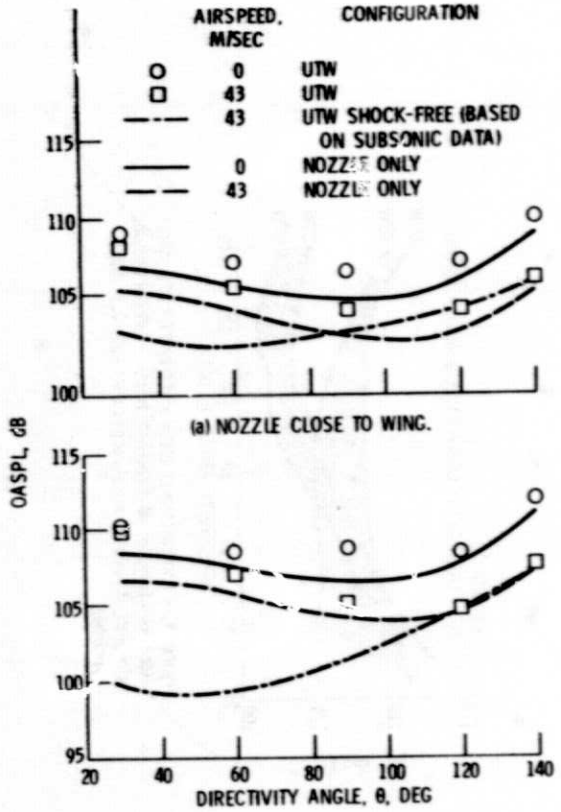

Figure 22. - Variation of OASPL with directivity angle for UTW configuration with conical nozzle. Flaps retracted.

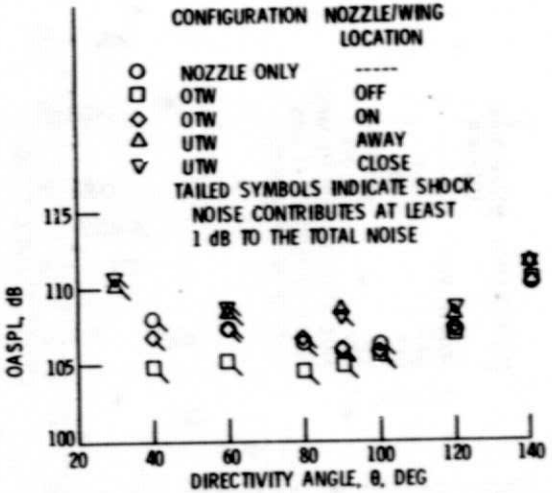

Figure 23. - Comparison of measured OASPL variation with directivity angle for EBF configurations. Free jet data; conical nozzle; flaps retracted; nozzle pressure ratio, 2.1; zero airspeed.

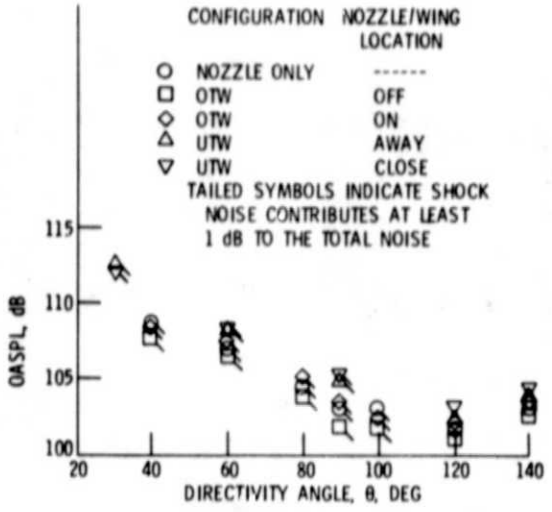

Figure 24. Comparison of airspeed effects on OASPL corrected for convective amplification as a function of directivity angle for various nozzle installations. Conical nozzle; flaps retracted; nozzle pressure ratio, 2.1; airspeed, 43 m/sec.

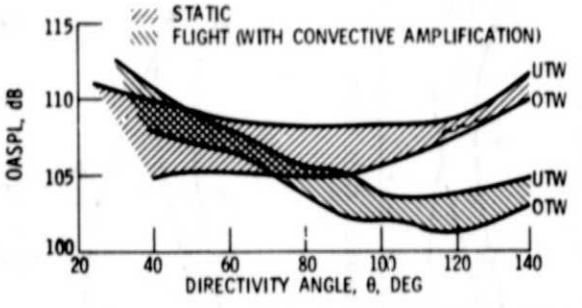

Figure 25. - Comparison of static and flight OASPL variations as a function of directivity angle. Conical nozzle; airspeed, 43 m/sec; nozzle pressure ratio, 2.1; flaps retracted.